References and Notes

1. G. E. Smith, G. A. Baraff, J. M. Rowell, *Phys. Rev.* **135**, A1118 (1964).
2. Yu. F. Komnik, E. I. Bukhshtab, Yu. V. Nikitin, V. V. Andrievskii, *Zh. Eksp. Teor. Fiz.* **60**, 669 (1971) [*Sov. Phys. JETP* **33**, 364 (1971)].
3. M. Lu *et al.*, *Phys. Rev. B* **53**, 1609 (1996).
4. J. H. Mangez, J-P. Issi, J. Heremans, *Phys. Rev. B* **14**, 4381 (1976).
5. Kai Liu, C. L. Chien, P. C. Searson, Kui Yu-Zhang, *Appl. Phys. Lett.* **73**, 1436 (1998).
6. Z. Zhang, X. Sun, M. S. Dresselhaus, J. Y. Ying, J. P. Heremans, *Appl. Phys. Lett.* **73**, 1589 (1998).
7. G. A. Prinz, *Science* **282**, 1660 (1998).
8. D. E. Beutler and N. Giordano, *Phys. Rev. B* **38**, 8 (1988).
9. D. L. Partin *et al.*, *ibid.*, p. 3818.
10. N. W. Ashcroft and N. D. Mermin, *Solid State Physics* (Saunders, Philadelphia, 1976), chap. 14.
11. F. Y. Yang *et al.*, unpublished data.
12. R. Schad *et al.*, *Appl. Phys. Lett.* **64**, 3500 (1994).
13. B. Dieny *et al.*, *Phys. Rev. B* **43**, 1297 (1991); T. C. Anthony, J. A. Burg, S. Zhang, *IEEE Trans. Magn.* **30**, 3816 (1994).
14. Supported by NSF grants DMR96-32526 and DMR97-32763.

13 January 1999; accepted 9 April 1999

Cracks Faster than the Shear Wave Speed

A. J. Rosakis,* O. Samudrala, D. Coker

Classical dynamic fracture theories predict the surface wave speed to be the limiting speed for propagation of in-plane cracks in homogeneous, linear elastic materials subjected to remote loading. This report presents experimental evidence to the contrary. Intersonic shear-dominated crack growth featuring shear shock waves was observed along weak planes in a brittle polyester resin under far-field asymmetric loading. When steady-state conditions were attained, the shear cracks propagated at speeds close to $\sqrt{2}$ times the material shear wave speed. These observations have similarities to shallow earthquake events where intersonic shear rupture speeds have been surmised.

Over the past 50 years, fracture mechanics theories have had enormous success in predicting the failure of brittle materials, a class of materials that exhibit a linear elastic constitutive response up to failure. Cracks or fractures are displacement discontinuities in an otherwise intact material. On the basis of the nature of the displacement discontinuity near the crack tip, three distinct fracture modes can be defined: mode I, the in-plane opening mode resulting from normal separation of the crack faces (opening displacement discontinuity); mode II, the in-plane shearing mode resulting from relative sliding of crack faces perpendicular to the crack edge (sliding displacement discontinuity); and mode III, the anti-plane shearing mode resulting from relative out-of-plane sliding of the crack faces (tearing displacement discontinuity).

Griffith's energy balance criterion states that if the body can supply sufficient energy per unit crack advance to the crack tip to create new surfaces, then crack initiation will take place. However, if a crack starts to propagate rapidly, inertial effects come into play and the kinetic energy of the material particles must be taken into account. Griffith's energy criterion is then appropriately modified to include the net flux of kinetic energy and elastic strain energy into a vanishingly small contour around the crack tip. As the crack tip speed is increased to the free surface or Rayleigh wave speed of the material, c_R, the net flux of energy into the propagating crack tip vanishes, thus making c_R the theoretical limiting crack tip speed (*1*). This speed is an upper bound for in-plane cracks in idealized continuum models without local length scales and structure. In real materials, experimentally observed crack tip speeds seldom exceed 40 to 50% of the Rayleigh wave speed even in the most brittle materials (*2, 3*). A variety of explanations, ranging from high strains (*4*) and micro damage zones around the crack tip (*3*) to wavy crack paths (*5*), have been offered to reconcile the discrepancy between the observed terminal speed and the theoretically determined limit.

Washabaugh and Knauss (*6*) proposed that the observed maximal speed of crack propagation is inherently related to the strength of the material. On the basis of earlier work by Ravichandar and Knauss (*3*), they argued that in amorphous brittle solids a zone of microcracks is generated around a propagating crack tip, which is responsible for substantially reducing the crack speed and eventually inducing crack tip branching. In their experiments, they suppressed the formation of microcracks and the tendency for branching by fabricating weak planes along which cracks were forced to propagate under remote, symmetric opening loading conditions. Along these weak planes they reported subsonic (speeds less than the shear wave speed, c_S) opening mode cracks with speeds asymptotically approaching $c_R \approx 0.92c_S$ in the limit of vanishing bond strength. In a laboratory setting, the only experimental observations of intersonic crack tip speeds (speeds between c_S and the dilatational wave speed, c_L) and supersonic crack tip speeds (speeds greater than c_L) have been limited to cases where the loading is applied directly at the crack tip. Winkler *et al*. reported supersonic crack growth along weak crystallographic planes in anisotropic single crystals of potassium chloride, where the crack tip was loaded by laser-induced expanding plasma (*7*). At an entirely different length scale, indirect observations of intersonic shear rupture have been reported for shallow crustal earthquakes (*8, 9*). Here the fault motion is primarily shear dominated, and the material is not strictly monolithic because preferred weak rupture propagation paths exist in the form of fault lines.

Motivated by the observations of highly dynamic shear rupture during earthquakes, a substantial analytical effort has been made to model the mechanics of both subsonic and intersonic dynamic shear crack propagation. Andrews (*10*) showed that a shear crack can have a terminal speed either less than c_R or slightly greater than $\sqrt{2}c_S$, depending on the cohesive strength of the fault plane ahead. Burridge *et al*. (*11*) concluded that the speed regime $c_S < v < \sqrt{2}c_S$ (where v is the crack tip speed) is inherently unstable for dynamic shear crack growth. Broberg (*12*) showed that the speed regime $c_R < v < c_S$ is forbidden for both opening and shear mode cracks, whereas the speed regime $c_S < v < c_L$ is forbidden for opening mode cracks only. Freund (*13*), on the basis of his asymptotic solution for a steady-state shear mode intersonic crack, concluded that $\sqrt{2}c_S$ is the only speed permissible for a stable intersonic shear crack. Broberg (*14, 15*) also solved the problem of an intersonic shear crack symmetrically expanding at constant speed from zero initial length. He allowed for the existence of a finite process region ahead of the tip and concluded that a shear crack can propagate at all intersonic speeds, except those close to c_S and c_L. He also discussed the importance of the speed $\sqrt{2}c_S$ within the assumptions of his model. All of these analytical studies constrained the shear crack to move along a prescribed straight-line path in its own plane. To our knowledge, direct experimental confirmation of intersonic shear crack growth has not yet been reported.

We sought to determine whether in-plane shear intersonic crack growth could be obtained in laboratory specimens under remote shear loading conditions. In monolithic, prenotched laboratory specimens subjected to shear loading, after initiation from the notch tip the crack does not follow a straight path in

Graduate Aeronautical Laboratories, California Institute of Technology, Pasadena, CA 91125, USA.

*To whom correspondence should be addressed. E-mail: rosakis@aero.caltech.edu

line with the notch; it invariably kinks in the local symmetric opening direction. To make shear crack growth possible by suppressing kinking, we introduced a weak plane ahead of the notch tip in the form of a bond between two identical pieces of isotropic material. The bonding process was carefully chosen so that the constitutive properties of the bond were close to those of the bulk material. We thus constructed a material system that, although not monolithic, can be considered homogeneous with regard to its linear elastic constitutive description. However, fracture toughness along the bond line is lower, so that the material is inhomogeneous with regard to its fracture properties. The notion of inhomogeneity in fracture toughness is not contained in any of the continuum models discussed above, which do not feature a fracture criterion. However, the weak bond line of the experimental specimens is equivalent to the straight-line crack path prescribed by these models.

Dynamic photoelasticity (Fig. 1) was chosen for capturing the stress field near the propagating crack tip because of its ability to visualize shear shock waves anticipated by the intersonic crack solutions. Two identical plates of Homalite-100, a brittle polyester resin that exhibits stress-induced birefringence, were bonded together and a notch was machined along the bond line at one edge. In addition, a number of specimens were also bonded by temperature-enhanced surface sintering (*6*), which does not involve any bonding agent. With this method there is no ambiguity regarding the constitutive homogeneity of the resulting bonded structure.

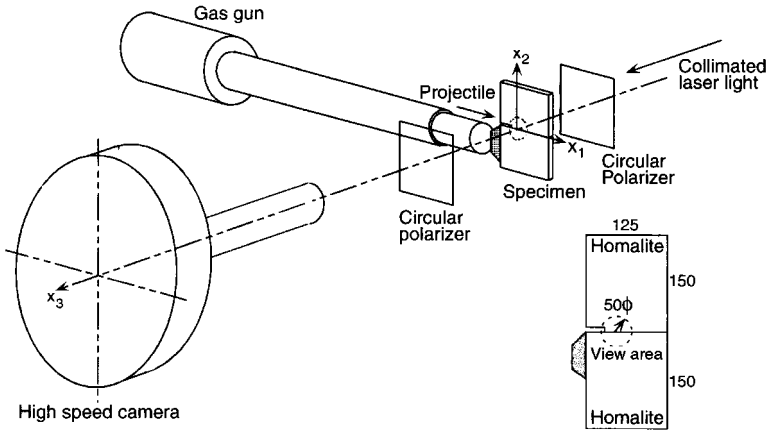

Fig. 1. The dynamic photoelasticity setup. A Homalite-100 (*29*) specimen is subjected to asymmetric impact by a projectile fired from a high-speed gas gun. The coordinate system (x_1, x_2, x_3) is centered at the crack tip. Dimensions are in millimeters. The specimen is 4 mm thick and the bond thickness is about 20 to 30 μm. The initial notch is 25 mm long and 2.3 mm wide. For Homalite-100, c_L = 2200 m/s and c_S = 1255 m/s. The steel projectile (length 75 mm, diameter 50 mm) impacts a steel piece, which was bonded to the specimen at the impact site to prevent shattering and to induce a planar loading wave front. The compressive longitudinal wave loads the notch tip in a predominantly shear mode. The dynamic stress field produced by the loading was recorded using photoelasticity in conjunction with high-speed photography. A coherent, monochromatic, plane-polarized, collimated laser beam (diameter ϕ = 50 mm) was transmitted through the specimen. The specimen was placed in a circular polariscope, and the resulting isochromatic fringe pattern was recorded by a rotating mirror-type high-speed camera capable of recording 80 frames at framing rates up to 2 million frames per second.

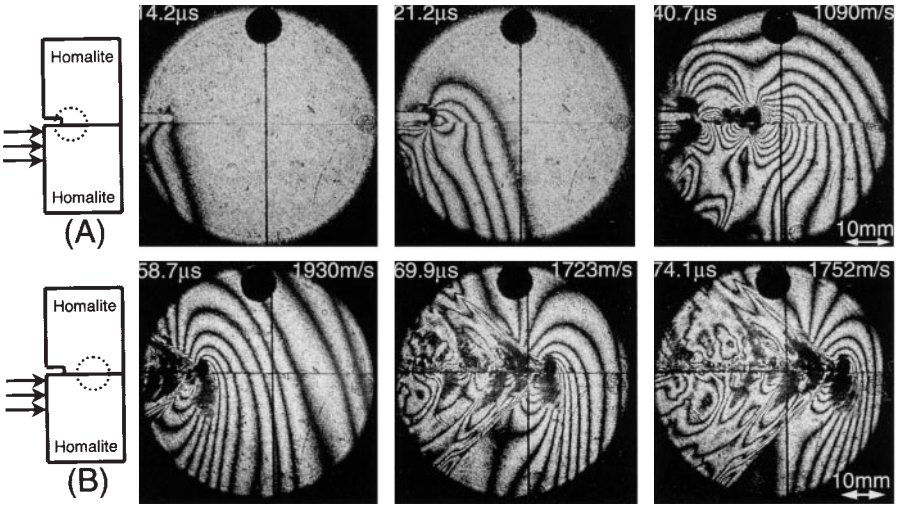

Fig. 2. Selected sequence of high-speed images showing the isochromatic fringe pattern around a propagating shear crack along a weak plane in Homalite-100. (**A**) Field of view enclosing the notch tip. (**B**) Field of view ahead of the notch tip. The frames included in the sequence are selected from two different experiments performed under identical conditions, except for the position of the field of view. Time after impact and crack tip speed are shown in each frame.

The specimen was subjected to asymmetric impact loading with a projectile at 25 m/s (Fig. 1). Sequences of isochromatic fringe patterns were recorded around a shear crack as it initiated and propagated along the interface between two Homalite halves (Fig. 2) (*16*). In Fig. 2A, the field of view encompasses the notch tip. The notch as well as the initial loading pulse are clearly visible in the first frame. The wave front is almost vertical, indicating that the notch is subjected to predominantly shear loading. In the next frame we see the wave diffraction around the notch tip and simultaneously observe the stress concentration building up. In the next frame we can discern a crack propagating dynamically along the interface after initiating from the notch tip. In Fig. 2B, the field of view is located downstream from the notch tip. In the first frame, we see a crack entering the field of view around which the shape of the isochromatic fringe pattern has changed drastically, and in the next frame we can clearly distinguish two lines radiating from the crack tip across which the fringe pattern changes abruptly (lines of shear stress discontinuity). These two lines correspond to the two traveling shear shock waves, which limit the spread of shear waves emanating from the crack tip as it propagates along the interface. The inclination of the shock waves indicates that the crack tip has exceeded the shear wave speed of Homalite, and has become intersonic. The fringe pattern around the propagating crack in the last frame is similar to that in the previous frame, indicating that the propagating crack has reached a steady state.

Crack tip speeds, v, were determined independently from the crack length history as well as from the inclination, β, of the shock waves to the crack faces ($v = c_S/\sin\beta$). From the crack tip speed histories in Fig. 3, we see that the initially recorded crack tip speed is close to the shear wave speed of Homalite (within experimental error of ±100 m/s) beyond which it accelerates (on the order of 10^8 ms^{-2}), thus becoming intersonic. Thereafter, it continues to accelerate up to the plane stress dilatational wave speed of Homalite, then decelerates and ultimately reaches a steady-state value of about $\sqrt{2}$ times the

shear wave speed. As seen in Fig. 2, the shock wave angle under steady-state conditions approaches an almost constant value around 43° to 45°, corresponding to a crack tip speed slightly higher than $\sqrt{2}c_S$. Recall that the speed regime between c_R and c_S is forbidden by theory on the basis of energy considerations (*12*). For this speed regime, the asymptotic solution predicts radiation of energy away from the crack tip (negative energy release rate), which is not possible on physical grounds. According to this rationale, a crack would have to jump discontinuously from the sub-Rayleigh regime to the intersonic regime. However, another possibility for generating such intersonic speeds is to bypass this forbidden regime by nucleating a crack from the initial notch that instantaneously starts to propagate at a speed above c_S. Within our experimental time resolution, the second scenario seems to be the most probable.

Freund's (*13*) asymptotic solution shows that unlike the subsonic case, the stress singularity exponent for an intersonically propagating shear crack tip is always less than 1/2, except at $v = \sqrt{2}c_S$, where it is equal to 1/2. This behavior implies that the energy flux into the crack tip (per unit crack advance) is zero in the intersonic regime, except at $v = \sqrt{2}c_S$ where it has a finite value. However, fracture processes essentially involve breaking of bonds and creation of new surfaces, which require a finite energy flow into the crack tip. This explains the behavior of the crack tip speed history in Fig. 3, where we saw the propensity of an intersonic mode II crack to propagate at a constant speed of $\sqrt{2}c_S$ under steady-state conditions. The stresses are also singular along the lines of discontinuity, with the same strength of singularity as that of the crack tip. The crack tip singularity is thus radiated away from the tip to create two singular shear shock waves.

An isochromatic fringe pattern recorded during our experiment (Fig. 4A) was compared with that predicted by theory (Fig. 4B) (*13*). The patterns are in good agreement with regard to the prediction of the two shock waves, their inclination to the crack faces, and the overall shape of the fringes. However, the experimental fringe pattern is distorted by the stress field generated by the loading pulse and possibly by crack face frictional contact.

In their opening mode experiments, Washabaugh and Knauss (*6*) observed that no matter how weak the crack propagation path, a symmetric opening (mode I) crack never exceeds c_R. This observation is consistent with the asymptotic solution, which predicts an unphysical radiation of energy (negative unbounded energy flux) away from the crack tip during opening mode intersonic crack propagation (*12*), thus excluding this crack growth scenario. However, as noted above, intersonic shear cracks are found theoretically to have a non-negative energy release rate; this allows the possibility of intersonic shearing mode crack growth, as confirmed experimentally here.

Dynamic shear crack propagation is of primary interest in modeling earthquake source dynamics. Analysis of far-field wave forms generated by shallow crustal earthquakes indicates that the source process represents a sudden stress drop across a rupture front, similar to a shear crack. Furthermore, the high pressures and temperatures deep inside Earth's crust rule out the existence of tensile cracks, allowing shear cracks only (*17–19*). The elastodynamic shear crack model provides an adequate approximation of the source process as a shear rupture along a preexisting weak fault plane whose function is equivalent to the weak bond line in our experiments. Average rupture speeds inferred for most of the shallow crustal earthquakes observed so far range from 0.7 to 0.9 c_S (*20*).

Rupture propagation is very sensitive to the properties of the surrounding material and as such is a highly transient process. Indeed, many large shallow earthquakes represent "multiple events" rather than the propagation of a single planar rupture front. Hence, for inferred average rupture speeds close to the shear wave speed, it is plausible that locally, for short durations, rupture speeds could be intersonic. Moreover, the local elastic wave speeds within the faults would be low relative to those of the bulk material typically reported in the literature. In such cases, a shear crack within the fault could go faster than local wave speeds and hence rupture could be locally intersonic. Archuleta (*8*) and Olsen *et al*. (*9*) suggested intersonic rupture velocities on the basis of their analyses of the strong motion data recorded during the 1979 Imperial valley earthquake and the 1989 Landers earthquake, respectively. Moreover, numerical studies on propagation of in-plane shear cracks (*10, 21*) have shown that, depending on the strength of the fault plane, propagation speeds can be either sub-Rayleigh or intersonic. Our current experiments have shown that intersonic rupture speeds are possible for shear cracks propagating along a prescribed weak plane. They also suggest that shear mode conditions near the crack tip are necessary to achieve intersonic crack tip speeds.

In the past, analytical predictions based on continuum theories have been made regarding the possibility of intersonic motion of other shear-dominated processes such as dislocation glide (*22–24*) and growth of mechanical twins (*25*). Intersonic glide of dislocations within the framework of discrete atomistic models was

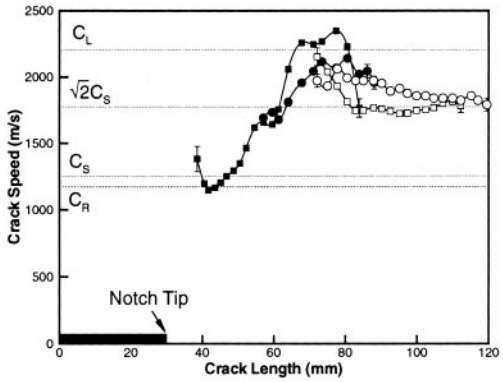

Fig. 3. Evolution of crack speed as the shear crack propagates along a weak plane in Homalite-100. Crack tip speed was obtained from crack length history (squares) and from shock wave angles (circles) for a field of view around the notch tip (solid symbols) and for a field of view ahead of the notch (open symbols).

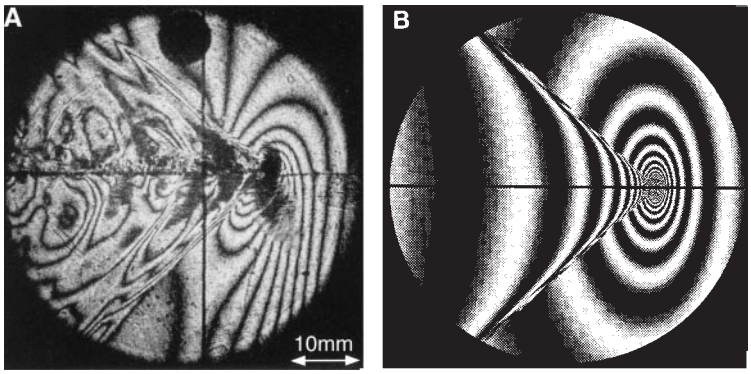

Fig. 4. Enlarged view of the isochromatic fringe pattern around a steady-state mode II intersonic crack along a weak plane in Homalite-100. (**A**) Experimental pattern. (**B**) Freund's theoretical prediction (*13*). For both cases, $\beta = 43°$ and $v = 1.47c_S$.

recently reported by Gumbsch and Gao (*26*). However, such processes, although similar to shear crack growth in the sense that they are driven by shear stresses, are also clearly different in the sense that they do not involve the breaking of material bonds and the subsequent creation of new surfaces. Moreover, no experimental confirmation of such intersonic processes is currently available. To date, our experimental observations of intersonic processes have been limited to cracks along bimaterial interfaces (*27*) and along the fibers in unidirectional composites (*28*). However, in both situations the crack speed was subsonic with respect to one of the two constituents, the material with higher wave speed in the case of bimaterials and the fibers in the case of unidirectional composites. The experiments presented here provide unambiguous evidence that shearing mode conditions near a propagating crack tip can drive the crack to intersonic speeds, which are found to be possible even in purely homogeneous systems with only one distinct set of wave speeds.

References and Notes

1. L. B. Freund, *Dynamic Fracture Mechanics* (Cambridge Univ. Press, Cambridge, 1990).
2. B. Cotterell, *Appl. Mat. Res.* **4**, 227 (1965).
3. K. Ravichandar and W. G. Knauss, *Int. J. Fract.* **26**, 141 (1984).
4. K. B. Broberg, *J. Appl. Mech.* **31**, 546 (1964).
5. H. Gao, *J. Mech. Phys. Solids* **1**, 457 (1993).
6. P. D. Washabaugh and W. G. Knauss, *Int. J. Fract.* **65**, 97 (1994).
7. S. Winkler, D. A. Shockey, D. R. Curran, *ibid.* **6**, 151 (1970).
8. R. J. Archuleta, *Bull. Seismol. Soc. Am.* **70**, 671 (1980).
9. K. B. Olsen, R. Madariaga, R. J. Archuleta, *Science* **278**, 834 (1997).
10. D. J. Andrews, *J. Geophys. Res.* **81**, 3575 (1976).
11. R. Burridge, G. Conn, L. B. Freund, *ibid.* **84**, 2210 (1979).
12. K. B. Broberg, *Int. J. Fract.* **39**, 1 (1989).
13. L. B. Freund, *J. Geophys. Res.* **84**, 2199 (1979).
14. K. B. Broberg, *Geophys. J. Int.* **119**, 706 (1994).
15. _____, *Arch. Mech.* **47**, 859 (1995).
16. The generation of the isochromatic fringe patterns, which are contours of constant maximum shear stress, is governed by the stress optic law, $nF/h = 2\tau_{max} = \sigma_1 - \sigma_2$, where F is the material fringe constant, h is the thickness of the specimen, σ_1 and σ_2 are the principal stresses, and n is the isochromatic fringe order.
17. J. R. Rice, in *Physics of the Earth's Interior*, A. M. Dziewonski and E. Boschi, Eds. (North-Holland, Amsterdam, 1980), pp. 555–649.
18. R. Dmowska and J. R. Rice, in *Continuum Theories in Solid Earth Physics*, R. Teisseyre, Ed. (Elsevier, Amsterdam, 1986), pp. 187–255.
19. S. Das, *Int. J. Fract.* **27**, 263 (1985).
20. H. Kanamori, D. L. Anderson, T. H. Heaton, *Science* **279**, 839 (1998).
21. S. Das and K. Aki, *Geophys. J. R. Astron. Soc.* **50**, 643 (1977).
22. J. D. Eshelby, *Proc. R. Soc. London Ser. A* **62**, 307 (1949).
23. J. Weertman, in *Mathematical Theory of Dislocations*, T. Mura, Ed. (American Society of Mechanical Engineers, New York, 1969), p. 178.
24. H. Gao, Y. Huang, P. Gumbsch, A. J. Rosakis, *J. Mech. Phys. Solids*, in press.
25. P. Rosakis and H. Tsai, *Int. J. Solids Struct.* **32**, 2711 (1995).
26. P. Gumbsch and H. Gao, *Science* **283**, 965 (1999).
27. A. J. Rosakis, O. Samudrala, R. P. Singh, A. Shukla, *J. Mech. Phys. Solids* **46**, 1789 (1998).
28. D. Coker and A. J. Rosakis, *Caltech SM Report 98-16* (1998).
29. Homalite-100, at room temperature, is well modeled as a linearly elastic material that is representative of a class of materials that undergo brittle fracture. Of particular importance is its property of birefringence that permits the use of the optical technique of photoelasticity for stress field mapping. The shear strength of bulk Homalite-100 is about 42 MPa, and the shear strength of the bond was systematically varied from 30 to 50% of the strength of the bulk material. This shear bond strength was measured with the use of a conventional Iosipescu shear test fixture.

30. Supported by NSF grant CMS9813100 and Office of Naval Research grant N00014-95-0453. A.J.R. thanks J. R. Rice of Harvard University for penetrating discussions during his November 1998 visit to Harvard. Helpful comments by B. Broberg of the University of Lund are also gratefully acknowledged.

17 December 1998; accepted 8 April 1999

Carbon Nanotube Actuators

Ray H. Baughman,[1]* Changxing Cui,[1] Anvar A. Zakhidov,[1] Zafar Iqbal,[1] Joseph N. Barisci,[2] Geoff M. Spinks,[2] Gordon G. Wallace,[2] Alberto Mazzoldi,[3] Danilo De Rossi,[3] Andrew G. Rinzler,[4] Oliver Jaschinski,[5] Siegmar Roth,[5] Miklos Kertesz[6]

Electromechanical actuators based on sheets of single-walled carbon nanotubes were shown to generate higher stresses than natural muscle and higher strains than high-modulus ferroelectrics. Like natural muscles, the macroscopic actuators are assemblies of billions of individual nanoscale actuators. The actuation mechanism (quantum chemical–based expansion due to electrochemical double-layer charging) does not require ion intercalation, which limits the life and rate of faradaic conducting polymer actuators. Unlike conventional ferroelectric actuators, low operating voltages of a few volts generate large actuator strains. Predictions based on measurements suggest that actuators using optimized nanotube sheets may eventually provide substantially higher work densities per cycle than any previously known technology.

The direct conversion of electrical energy to mechanical energy through a material response is critically important for such diverse needs as robotics, optical fiber switches, optical displays, prosthetic devices, sonar projectors, and microscopic pumps. Ferroelectric and electrostrictive materials are especially useful for direct energy conversion. However, applications are restricted by the maximum allowable operation temperature, the need for high voltages, and limitations on the work density per cycle.

Conducting polymer actuators based on electrochemical dopant intercalation were proposed a decade ago (*1*) and have been pioneered in many different laboratories (*2*, *3*). Faradaic processes for these batterylike devices involve solid-state dopant diffusion and structural changes that limit rate, cycle life, and energy conversion efficiencies.

The new actuators we describe here use carbon single-walled nanotube (SWNT) sheets (*4*) as electrolyte-filled electrodes of a supercapacitor. No dopant intercalation is required for device operation. Changing the applied voltage injects electronic charge into a SWNT electrode, which is compensated at the nanotube-electrolyte interface by electrolyte ions (forming the so-called double layer). The new actuators use dimensional changes in covalently bonded directions caused by this charge injection, which originate from quantum chemical and double-layer electrostatic effects. For low charge densities, calculations (*5*) and experimental results (*6*) for charge transfer complexes of graphite and conducting polymers (Fig. 1) show that the strain due to quantum mechanical effects (changes in orbital occupation and band structure) changes sign from an expansion for electron injection to a contraction for hole injection. However, expansion results from both quantum chemical effects and electrostatic double-layer charging for high-density charge injection of either sign (*5*, *6*).

Like natural muscle (*7*), the nanotube sheet actuators are arrays of nanofiber actuators. A novel type of actuation results because the SWNTs add high surface area to the mechanical properties, electrical conductivity, and charge transfer properties of graphite. The results presented here are for nanotube sheets ("nanotube paper") composed of mats of nanotube bundles joined by mechanical entangle-

[1]Research and Technology, AlliedSignal, 101 Columbia Road, Morristown, NJ 07962–1021, USA. [2]Intelligent Polymer Research Institute, University of Wollongong, New South Wales 2522, Australia. [3]School of Engineering, University of Pisa, Centro E. Piaggio, Via Diotisalvi, 2–56100 Pisa, Italy. [4]Department of Physics, University of Florida, Gainesville FL 32611–8440, USA. [5]Max Planck Institut für Festkoerperforschung, Heisenbergstrasse 1, D-70569 Stuttgart, Germany. [6]Department of Chemistry, Georgetown University, Washington, DC 20057–1227, USA.

*To whom correspondence should be addressed. E-mail: ray.baughman@alliedsignal.com